

Anyon Bosonization of 2D Fermions and Single Boson Phase Diagram Implied from Experiment on Visualizing Pair Formation in Superconductor $Bi_2Sr_2CaCu_2O_{8+\delta}$

B. Abdullaev^{1,2}, C. -H. Park², and M. M. Musakhanov¹

Physics, National University of Uzbekistan, Tashkent 100174, Uzbekistan.

²*Research Center for Dielectric and Advanced Matter Physics, Department of Physics, Pusan National University, 30 Jangjeon-dong, Geumjeong-gu, Busan 609-735, Korea.*

(Dated: Received November 21, 2018)

Recently, Gomes *et al.* [1] have visualized the gap formation in nanoscale regions (NRs) above the critical temperature T_c in the high- T_c superconductor $Bi_2Sr_2CaCu_2O_{8+\delta}$. It has been found that, as the temperature lowers, the NRs expand in the bulk superconducting state consisted of inhomogeneities. The fact that the size of the inhomogeneity [2] is close to the minimal size of the NR [1] leads to a conclusion that the superconducting phase is a result of these overlapped NRs. In the present paper we perform the charge and percolation regime analysis of NRs and show that at the first critical doping x_{c1} , when the superconductivity starts on, each NR carries the positive electric charge one in units of electron charge, thus we attribute the NR to a single hole boson, and the percolation lines connecting these bosons emerge. At the second critical doping x_{c2} , when the superconductivity disappears, our analysis demonstrates that the charge of each NR equals two. The origin of x_{c2} can be understood by introducing additional normal phase hole fermions in NRs, whose concentration appearing above x_{c1} increases smoothly with the doping and breaks the percolation lines of bosons at x_{c2} . The last one results in disappearing the bulk bosonic property of the pseudogap (PG) region, which explains the upper bound for existence of vortices in Nernst effect [3]. Since [1] has demonstrated the absence of NRs at the PG boundary one can conclude that along this boundary, as well as in x_{c2} , all bosons disappear. As justification of appearance of single bosons, the bosonization of 2D fermions is rigorously proven using the concept of anyons. The linear density dependence of the energy gap between excited fermionic and bosonic ground states describes the Uemura relation for 2D superconductors.

PACS numbers: 74.20.De, 74.25.Dw, 74.72.Gh, 74.72.Kf

I. INTRODUCTION

The origin of PG and high-temperature superconductivity phases in copper oxides is the most puzzling and challenging problem in condensed matter physics. Despite on the intensive experimental and theoretical studies we have no clear understanding of these phases so far. A relationship between two phases has become a subject of wide range theoretical proposals and their possible experimental testing. A precursor scenario for the PG state supposes pairing correlations without superconducting phase coherence [4]. This scenario has been confirmed by experiments [3, 5]. A description for the PG phase based on the electronic competing order mechanism with experimental arguments was given in [6]. Other observations have associated the PG with a real space electronic organization [7] which is dominant at low dopings.

The fundamental property of the PG is a partial gap in the density of states [8] which is observed in various experiments. To understand the nature of this gap the real space atomic scale scanning tunneling microscopy measurements of the copper oxide $Bi_2Sr_2CaCu_2O_{8+\delta}$ have been performed. For the case of high- T_c superconductiv-

ity the spatial gap inhomogeneities have been observed in [9, 10], while Pan *et al.* [2] explicitly determine their minimal size. The evolution of the nanoscale gap formation with temperature decrease in the PG region has been investigated by Gomes *et al.* [1].

In the present paper we study the origin of minimal size NRs, which were visualized in Refs. [1, 2] through the measurement of the energy gap. We use the experimental fact that PG and superconductivity phases are formed from the NRs. Particularly, we are interested in the electric charge of NRs. We will employ the information about the charge to understand some ingredients of doping-temperature phase diagram of $Bi_2Sr_2CaCu_2O_{8+\delta}$ copper oxide. The generalization of our consideration to other cuprates will be given as well. It is worth to notice that all physical findings in the paper are inferred from the analysis of data for the NRs in [1, 2]. The most important fermionic nature of the second hole inside NR at x_{c2} and dopings below x_{c2} is implied from the meaning of the second critical doping x_{c2} : at this doping the superconductivity and hence, the bosonic property of the matter disappears. The justification of the appearance of single hole bosons will be given using the concept of anyons.

In such a treatment the anyon vector potential and the corresponding statistical magnetic field represent Berry connection and fictitious magnetic field [11], respectively. A significant role of the fictitious magnetic field, as a real quantity originated from the Berry phase, has been stressed in Refs. [12, 13] in the non-pairing mechanism of high- T_c superconductivity. We will demonstrate that $2D$ fermions can be bosonized. So that the fermion ground state becomes an excited state with respect to the boson one. The linear density dependence of the energy gap between these two states describes the well-known Uemura relation for $2D$ superconductors.

In Sec. II we describe the charge and percolation analysis of NRs on the base of experimental data given in Refs. [1] and [2]. The analysis provides the interpretation of some elements of the phase diagram doping-temperature in $Bi_2Sr_2CaCu_2O_{8+\delta}$ compound. Sec. III is devoted to a rigorous proof of the bosonization of $2D$ fermions and existence of the bosonic ground state for any $2D$ quantum system. Another implication of the bosonization to investigation of the universal Uemura relation for $2D$ superconductors is outlined in Sec. IV. We summarize and conclude our paper in Sec. V.

II. EXPERIMENT IMPLIED SINGLE BOSON PHASE DIAGRAM

The authors of Ref. [1] have visualized the NRs in the PG region of $Bi_2Sr_2CaCu_2O_{8+\delta}$ compound at fixed hole dopings $x = 0.12, 0.14, 0.16, 0.19, 0.22$. It has been determined that for $x = 0.16$ and $x = 0.22$ the minimal size of the NRs is $\xi_{coh} \approx 1 - 3$ nm. The estimated minimal size of NRs, ξ_{coh} , is about 1.3 nm in the superconducting phase [2] ($T_c = 84K$). Another notable result obtained in Ref. [2] is the observation of spatial localization of the doped charges. The charges are localized in the same area as NRs [2] with the same coherence length ξ_{coh} . Below we will demonstrate that the next spatial parameter, the mean distance between two holes, r_0 , is important to understand the underlying physics. The experimental doping dependence of r_0 can be approximated by the relationship $r_0 \approx a/x^{1/2}$ (see Fig. 34 in Ref. [14]), where a is a lattice constant in the elementary structural plaquette for the CuO_2 $a - b$ plane of a copper oxide. This relationship is derived in Ref. [14] for $La_{2-x}Sr_xCuO_4$ compound with $a \approx 3.8\text{\AA}$. It is valid for our compound as well since the lattice constant a of $Bi_2Sr_2CaCu_2O_{8+\delta}$ is $a \approx 3.8\text{\AA}$ (see the capture to Fig.2 in Ref. [10]). It is worth to mention that $b \approx a$ for the lattice constant b of the same structural plaquette.

A principal part of our analysis is the doping x dependence of the NR charge $(\xi_{coh}/r_0)^2$. We start with a case of zero temperature. The parameter ξ_{coh}/r_0 contains an essential information in our consideration. The factor $(\xi_{coh}/r_0)^2$ reduces to the expression $x(\xi_{coh}/a)^2$ which has a simple physical meaning: it is a total electric charge of $(\xi_{coh}/a)^2$ number of plaquettes each of them having a

charge x . On the other hand, the parameter ξ_{coh}/r_0 describes the average spatial overlapping degree of two or more holes by one NR. If $\xi_{coh}/r_0 > 1$ then all NRs will be in close contact to each other providing by this the bulk superconductivity in percolation regime.

In the Table I we outline the doping x dependencies for the function $(\xi_{coh}/r_0)^2$ for fixed experimental values $\xi_{coh} = 10\text{\AA}$ (the minimal size of the NR) and $\xi_{coh} \approx 13\text{\AA}$ taken from Ref. [1] and Ref. [2], respectively, and for the function ξ_{coh} which fits $(\xi_{coh}/r_0)^2$ to $(10\text{\AA}/r_0)^2$ at $x = 0.28$ and for $x = 0.05$ provides $(\xi_{coh}/r_0)^2 \approx 1.0$. Numerical values of the ξ_{coh}/r_0 are also shown in the table.

Since in Ref. [1] every NR location in the sample is tracked with the precision 0.1\AA , we suppose that the $\xi_{coh} = 10\text{\AA}$ has been measured with a high enough accuracy. In addition, we assume that in Ref. [2] the $\xi_{coh} \approx 13\text{\AA}$ is measured with the same accuracy at $x = 0.14$. Under this condition, we conclude that the tendency of ξ_{coh} to growth from 10\AA to 13\AA when x decreases from 0.22 to 0.14 reflects quantitatively the underlying physics. The data for the resulting parameter ξ_{coh}/r_0 is approximated by the function $2.2x^{1/3}$. The analytic equation for ξ_{coh} expressed in terms of the lattice constant a is given by $\xi_{coh} \approx 2.2a/x^{1/6}$.

As seen from Table I, the charges $(10\text{\AA}/r_0)^2$, $(13\text{\AA}/r_0)^2$, and $(\xi_{coh}/r_0)^2$ vary continuously with the doping x . This is not surprising because they are functions of $r_0(x)$ and $\xi_{coh}(x)$. From the analysis at the first critical doping, $x_{c1} = 0.05$, it follows that the charge $(\xi_{coh}/r_0)^2$ of the visualized NR in Ref. [1] equals +1. So that, it corresponds to the charge of a single hole. Notice, at the critical doping $x_{c1} = 0.05$ the percolation parameter is given by $\xi_{coh}/r_0 = 1.0$. That means the whole sample is entirely covered with mini areas $\xi_{coh}^2 = r_0^2$ contacting each other. It is unexpected that at the second critical doping, $x_{c2} = 0.28$, the charge of the visualized NR takes the value +2. This implies that at $\xi_{coh}^2 = 2r_0^2$ one has a pair of holes inside the NR and, as a result, the superconductivity disappears completely. For $x_{c2} = 0.28$ we have $\xi_{coh}/r_0 > 1.0$, so that the charge conductivity of the fermions still remains.

Notice, that there are no particles in the nature with the fractional charge, except the quasiparticles which can be produced by many-body correlations like in the fractional quantum Hall effect [15]. Hence, the problem of the presence of the extra fractional charge inside the NR has to be solved yet. We remind [1, 2] that PG visualized NRs constitute the bulk superconductivity phase below the critical temperature T_c , and therefore, they are a precursor for that phase. This implies undoubtedly that the NRs represent bosons at least. At $x_{c1} = 0.05$ one has the charge $(\xi_{coh}/r_0)^2 = 1$, so that one may conjecture that the NR represents just a boson localized in the square box ξ_{coh}^2 .

For $x > 0.05$ the charge $(\xi_{coh}/r_0)^2$ has an additional to +1 fractional part. We assign the last one to the fractional part of the charge of fermion. Thus the total

charge $(\xi_{coh}/r_0)^2$ of the NR includes the charge +1 of the boson and the fractional charge of the fermion. However, as it was mentioned above, the fractional charge can not exist. Therefore, we take the number N_{ob} of NRs to be equaled to the inverse value of the fractional part to form a charge +1 of the fermion. As a result, we obtain one fermion surrounding by N_{ob} bosons. The values of N_{ob} are outlined in the last column of the Table 1.

The NRs introduced in such a manner allow to understand clearly the evolution of the fermions in the whole range $0.05 \leq x \leq 0.28$ of doping and to explain the origin of the second critical doping $x_{c2} = 0.28$. It is clear, as x increases, the number of fermions grows up inside the superconducting phase. By this, at x_{c2} , when the number of fermions becomes equal to the number of bosons, one has the breaking of the boson percolation lines, and, thus the superconductivity disappears.

It is worthwhile to compare ξ_{coh} with the lattice constant a of $Bi_2Sr_2CaCu_2O_{8+\delta}$ compound when the doping x varies. We have $2.6a \leq \xi_{coh} \leq 4.5a$ for variation of x from x_{c2} to x_{c1} . However, it is well known that the antiferromagnetic dielectric parent materials are characterized by a strong short range magnetic interaction within the atomic length scale a . Therefore, one may assume that a is a length parameter for these compounds. The fact that the size ξ_{coh} is larger than $2.6a$ leads to a conclusion that the visualized NRs are independent from the dielectric environment (the latter forms only the spatial square shape of the NR). Due to this, the numerical values $x_{c1} = 0.05$ and $x_{c2} = 0.28$ are universal for all hole doped cuprates. However, at the second critical doping x_{c2} the length scale of boson and fermion (the half of ξ_{coh}) inside NR is comparable to a . Therefore, the parent compound starts to play a role from the critical doping x_{c2} . Furthermore, since a coincidence of x_{c2} with the PG boundary at a zero temperature has been observed in various experiments and for all temperatures of this boundary no NRs, which exhibit gaps, were detected [1], the plausible intuitive finding would be the total disappearance of bosons along the PG bound line. So that two fundamental phenomena – the breaking of the boson percolation lines and the disappearance of bosons – occur at x_{c2} . The first phenomenon indicates the end of the bulk bosonic property and the end of the T_c curve as well, whereas the second phenomenon corresponds to the end of the bosonic property in general. For the PG region the disappearance of the bulk bosonic property was detected by observing the onset temperature, T_{onset} , for the existence of vortices in the Nernst effect [3]. The vortices have been seen so far only in quantum Bose systems. Further evolution of fluctuations with temperature increase destroys the bosons which totally vanish at PG boundary.

The schematic single hole bosonic phase diagram for $Bi_2Sr_2CaCu_2O_{8+\delta}$ is depicted in the Fig. 1. The coloured zones indicate the percentage of the sample that is gapped at given temperature and doping (in analogy with the phase diagram shown in Ref. [1]). The solid lines

x	$(10\text{\AA}/r_0)^2$	$(13\text{\AA}/r_0)^2$	$\xi_{coh}(\text{\AA})$	$(\xi_{coh}/r_0)^2$	ξ_{coh}/r_0	N_{ob}
0.28	1.939	3.277	10	1.939	1.393	~ 1
0.22	1.524	2.575	10	1.524	1.235	~ 2
0.16	1.108	1.873	11	1.341	1.158	~ 3
0.14	0.969	1.638	12	1.396	1.182	~ 3
0.10	0.693	1.170	13	1.170	1.082	~ 6
0.05	0.346	0.585	17	1.000	1.000	
0.04	0.277	0.468	18	0.897	0.947	
0.02	0.139	0.234	20	0.554	0.744	

TABLE I: The doping x dependencies of NR charges. The doping x dependencies for $(10\text{\AA}/r_0)^2$, $(13\text{\AA}/r_0)^2$ at fixed $\xi_{coh} = 10\text{\AA}$ and $\xi_{coh} = 13\text{\AA}$, respectively, for the coherent length ξ_{coh} , the charge $(\xi_{coh}/r_0)^2$ and the percolation parameter ξ_{coh}/r_0 at this ξ_{coh} are presented. The values for the number N_{ob} of bosons surrounding every fermion are shown in the last column.

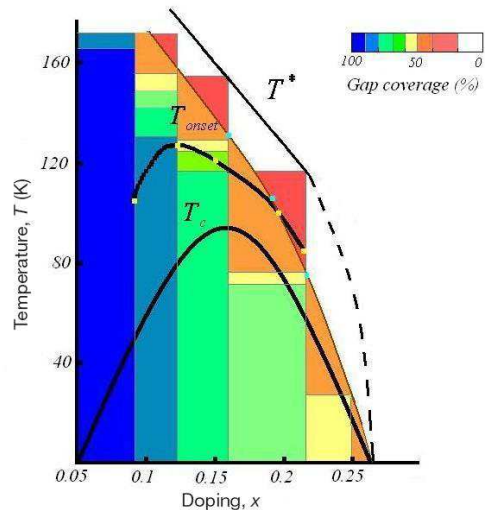


FIG. 1: Schematic single hole bosonic phase diagram for $Bi_2Sr_2CaCu_2O_{8+\delta}$.

correspond to the following observed temperatures: PG boundary T^* and onset temperature T_{onset} for Nernst effect signals taken from Ref. [3], and the critical temperature T_c from Ref. [1]. The extrapolation of the connection of T^* with the second critical doping, x_{c2} , is depicted by the dashed line. The yellow points correspond to fixed T_{onset} values from Ref. [3], and the blue points represent the temperature data for 50% of gapped area of the sample from Ref. [1] measured at fixed dopings. The thin brown coloured solid line fits the blue points. The percentage for the gapped doping is calculated by using the equation $(1 - 1/(N_{ob} + 1)) \cdot 100\%$ under the assumption that the NRs overlap each other. It is remarkable that T_{onset} line is substantially located in the brown coloured

zones which means there is no bulk bosonic property above these zones. It is worth to compare the homogeneous 100% gap coverage observed in Ref. [1] with our proposed varying one in Fig. 1 for low temperature and doping levels $0.12 \leq x \leq 0.22$. Employing the doping changing dynamics of the 50% gap coverage obtained in Ref. [1], we find that this percentage is applicable also at the second critical doping, x_{c2} , which is shown in Fig. 1 by yellow (60%) and brown (50%) colours. On the other hand, if we consider the NR charge +1 for the above interval of doping with further its increasing up to +2, close to x_{c2} , then we will reproduce exactly the percentages observed in the phase diagram in Ref. [1].

The next interesting finding is that the number of external interstitial atoms sufficient to produce one doped hole in the dielectric parent material equals to $1/x$. For $La_{2-x}Sr_xCuO_4$ compound it is a number of Sr atoms, since the hole doping and the concentration of atoms are expressed by x . In the interval $0.05 \leq x \leq 0.28$ this number varies from 20 to 3.

At the end of this section, we discuss on the percolation threshold of 2D classical systems and compare it with our 50% one used for bulk bosonic property. If we remind white and black cells of the chessboard and assume that the black ones represent a region in which the percolation should occur, it becomes clear that the percolation threshold consists of 50% coverage by this colored region of the whole chessboard area. The experiment for some particular system indicates to more than 40% coverage for its value [16] (the numerical simulation for the same system has confirmed this observed result [17]).

III. REAL BOSONIZATION OF 2D FERMIONS

It might be seem that the appearance of the single hole bosons in the real matter is too exotic and never can be realized. Since it is hard even to imagine that except a pairing of fermions, as in conventional superconductors, some other mechanisms can lead to transformation of fermions into bosons. However, the fact that $a-b$ planes of CuO_2 atoms play a dominant role in the determination of the physics of cuprates provides an opportunity to exploit the fundamental property of the two-dimensionality. Specifically, the 2D topology allows the fractional statistics [18] characterized by a continuous parameter ν taking values between 0 (for bosons) and 1 (for fermions). The particles with $0 < \nu < 1$ are generically called anyons [19, 20]. The quasiparticle excitations in the fractional quantum Hall regime [21–23] and in certain quantum magnets [24] can be described using the anyon concept. One can apply the last one in the study of properties of the mentioned above $a-b$ planes.

In this section we will present the rigorous derivation of the real bosonization of 2D fermions. It can be achieved by exact cancellation of terms in the ground state energy arisen from fermion (anyon) statistics and a Zeeman interaction of spins $\hbar/2$ of particles with statistical

magnetic field [22, 25] produced by vector potential of anyons. As in our recent papers [26, 27], the calculation will be carried out in the framework of a variational approach. However, we do not use the cut-off regularization procedure of the logarithmic divergence for the nearest interparticle distance, as it was done in [26], since the short-range correlations of particles will be accurately taken into account in the system wave function. In [28] the bosonization of 2D fermions has been obtained approximately using the cut-off regularization.

Let us consider the Hamiltonian

$$\hat{H} = \frac{1}{2M} \sum_{k=1}^N \left[\left(\vec{p}_k + \vec{A}_\nu(\vec{r}_k) \right)^2 + M^2 \omega_0^2 |\vec{r}_k|^2 \right] + \frac{1}{2} \sum_{k=1}^N \left[V(\vec{r}_k) + \sum_{j \neq k}^N \frac{e^2}{|\vec{r}_{kj}|} \right] \quad (1)$$

of the gas of N anyons with mass M and charge e , confined in 2D parabolic well, interacting through Coulomb repulsion potential in the presence of uniform positive background [15] $V(\vec{r}_k)$. Here, \vec{r}_k and \vec{p}_k represent the position and momentum operators of the k th anyon in 2D space dimension,

$$\vec{A}_\nu(\vec{r}_k) = \hbar\nu \sum_{j \neq k}^N \frac{\vec{e}_z \times \vec{r}_{kj}}{|\vec{r}_{kj}|^2} \quad (2)$$

is the anyon gauge vector potential [29], $\vec{r}_{kj} = \vec{r}_k - \vec{r}_j$, and \vec{e}_z is the unit vector normal to the 2D plane. In the expression for $\vec{A}_\nu(\vec{r}_k)$ and hereafter we assume that $0 \leq \nu \leq 1$.

In the bosonic representation of anyons we take the system wave function in the form [30] (see also [31]):

$$\Psi(\vec{R}) = \prod_{i \neq j} r_{ij}^\nu \Psi_T(\vec{R}). \quad (3)$$

Here $\vec{R} = \{\vec{r}_1, \dots, \vec{r}_N\}$ is the configuration space of the N anyons. The product in the right hand side of this equation is the Jastrow-type wave function. It describes the short distance correlations between two particles due to anyonic (fermionic) statistics interaction.

Let us consider first the term in the Hamiltonian \hat{H} , Eq. (1) containing the anyon vector potential $\vec{A}_\nu(\vec{r}_k)$. Substituting $\Psi(\vec{R})$, Eq. (3), in Schrodinger equation with this Hamiltonian, we obtain an equation $\tilde{H}\Psi_T(\vec{R}) = E\Psi_T(\vec{R})$ with the novel Hamiltonian $\tilde{H} = \tilde{H}_1 + \tilde{H}_2$, where

$$\tilde{H}_1 = \sum_{k=1}^N \left(\frac{-\hbar^2 \Delta_k}{2M} - \frac{\hbar^2 \nu}{M} \sum_{j \neq k}^N \frac{\vec{r}_{kj} \cdot \vec{\nabla}_k}{|\vec{r}_{kj}|^2} \right) \quad (4)$$

and

$$\tilde{H}_2 = -i \frac{\hbar}{M} \sum_{k=1}^N \left(\vec{A}_\nu(\vec{r}_k) \cdot \vec{\nabla}_k + \nu \sum_{j \neq k}^N \frac{\vec{A}_\nu(\vec{r}_k) \cdot \vec{r}_{kj}}{|\vec{r}_{kj}|^2} \right). \quad (5)$$

As shown in Ref. [30], the ν interaction Hamiltonian in \tilde{H}_1 , i.e., the second its term, is equivalent to a sum of two-body potentials

$$\frac{\pi\hbar^2\nu}{M} \sum_{j \neq k} \delta^{(2)}(\vec{r}_k - \vec{r}_j). \quad (6)$$

Therefore, the Hamiltonian \tilde{H}_1 now reads

$$\tilde{H}_1 = \sum_{k=1}^N \left(\frac{-\hbar^2\Delta_k}{2M} + \frac{\pi\hbar^2\nu}{M} \sum_{j \neq k} \delta^{(2)}(\vec{r}_k - \vec{r}_j) \right). \quad (7)$$

The wave function $\Psi(\vec{R})$ has been used in Refs. [30] and [31] in approximate perturbative treatment for the calculation of the ground state energy close to boson end of anyons $\nu \rightarrow 0$. Being calculated without the Jastrow product constituent, this energy displays the logarithmic divergence problem in regard to the nearest interparticle distance on which we already mentioned above.

To check the quality of $\Psi(\vec{R})$ for the entire range of the anyon parameter ν we consider the system of harmonically confined anyons without Coulomb interaction and calculate its ground state energy. To do this we add the parabolic potential $M\omega_0^2|\vec{r}_k|^2/2$ inside the brackets in Eq. (7) thus redefining the Hamiltonian \tilde{H}_1 .

In the variational scheme [26] we minimize the expression

$$E = \frac{\int \Psi_T^*(\vec{R}) \tilde{H} \Psi_T(\vec{R}) d\vec{R}}{\int \Psi_T^*(\vec{R}) \Psi_T(\vec{R}) d\vec{R}}. \quad (8)$$

For energies expressed in units of $\hbar\omega_0 = \hbar^2/(ML^2)$ and lengths in units of L the normalized trial wave function has the following form

$$\Psi_T(\vec{R}) = \left(\frac{\alpha}{\pi}\right)^{N/2} \prod_{k=1}^N \exp\left(-\alpha \frac{(x_k^2 + y_k^2)}{2}\right). \quad (9)$$

Here, α is the variational parameter.

The simple calculation shows that the expectation value E with the Hamiltonian \tilde{H}_2 , Eq. (5), and wave function given by Eq. (9), equals zero. Therefore, we will assume in Eq. (8) $\tilde{H} = \tilde{H}_1$.

A minimization of the energy E with respect to α gives the expression for the ground state energy

$$E_0 = \hbar\omega_0 N(1 + \nu(N-1))^{1/2}, \quad (10)$$

which coincides exactly with Eq. (21) in our paper [26] found by using the cut-off regularization. In Ref. [26] we have compared the exact numeric values for the ground state energy of fermions in the harmonic potential obtained by using the Pauli exclusion principle with ones calculated by using the Eq. (10) for $\nu = 1$. As demonstrated in Figs. 1 and 2 of [26], the maximal deviation

(no more than 12%) occurs at small numbers of N and this deviation tends to zero for increasing N . For large N and arbitrary ν the formula (10) is consistent (up to a numerical factor) with the approximate expression $E \approx \hbar\omega_0\nu^{1/2}N^{3/2}$ of Chitra and Sen [32] calculated in Thomas-Fermi approximation for $\nu > 1/N$. It is obvious that Eq. (10) reproduces the result of Wu (see the paper of Wu in Refs. [29]) in the bosonic limit $\nu \rightarrow 0$. This analysis unambiguously shows that the Hamiltonian \tilde{H}_1 , Eq. (7), reproduces accurately the anyon statistics interaction for all values of ν and N (there is no doubt that the harmonically confinement potential does not affect on the statistics interaction).

Now we demonstrate the real bosonization of 2D fermions on the example of anyons in parabolic well. To do this we consider the Zeeman interaction term

$$\frac{\hbar}{M} \sum_{k=1}^N \hat{s} \cdot \vec{b}_k \quad (11)$$

of spins with the statistical magnetic field [25] (see also [22])

$$\vec{b}_k = -2\pi\hbar\nu\vec{e}_z \sum_{j \neq k} \delta^{(2)}(\vec{r}_k - \vec{r}_j), \quad (12)$$

which can be derived if one calculates $\vec{b}_k = \vec{\nabla} \times \vec{A}_\nu(\vec{r}_k)$ by using Eq. (2).

The sign in Eq. (11) is taken according to the standard definition $-\vec{\mu}\vec{H}$ of the Zeeman term [33], where $\vec{\mu}$ and \vec{H} are a magnetic moment of a spin and an external magnetic field, respectively. It takes into account also self consistently the charge sign of particles and direction of the statistical magnetic field \vec{b}_k . For electrons with charge $e = -|e|$ adopted in this paper the condition $\nu > 0$ is correct, while for holes with charge $e = |e|$ one needs to take $\nu = -|\nu|$ in the expression for \vec{b}_k , and to change the sign of Eq. (11) itself. In the last case one has to replace ν with $|\nu|$ in all our formulas below.

For $s_z = \hbar/2$ and using the expression, Eq. (12), for \vec{b}_k one obtains

$$\frac{\hbar}{M} \sum_{k=1}^N \hat{s} \cdot \vec{b}_k = -\pi\nu \frac{\hbar^2}{M} \sum_{k(j \neq k)} \delta^{(2)}(\vec{r}_k - \vec{r}_j). \quad (13)$$

Being added to the expression, Eq. (7), for the Hamiltonian \tilde{H}_1 , this Zeeman term cancels exactly the second one of \tilde{H}_1 , which is responsible for the statistics of fermions (for $\nu = 1$) and anyons. Since the energy of bosons is lower than one for fermions and anyons, there appears a coupling of spin with statistical magnetic field for every particle or bosonization of 2D fermions and anyons. From this one can conclude, if anyon concept is correct for the description of any 2D quantum system, its ground state should be bosonic with $\nu = 0$, while its excited state should be fermionic ($\nu = 1$) or anyonic ($0 < \nu < 1$) depending of the fixed value of ν .

It might seem that the subject described in this section has no relation to real physics since the physical sense of the statistical magnetic field is unclear or may have an artificial meaning. However, if we express the gauge vector potential $\vec{A}_\nu(\vec{r}_k)$, Eq. (2), in the form $\vec{A}^{fic} = \hbar\nu\nabla_{2D}\chi$, where the expression of the angular variable χ , Eq. (3) of Ref. [11], is exactly coincides with one for anyons, Eq. (3.2.31) of book [22], it becomes evident that $\vec{A}_\nu(\vec{r}_k)$ represents the Berry connection and the statistical magnetic field is the fictitious magnetic field originated from the Berry phase [11] of anyons (see book of Wilczek [20]). As it was demonstrated in Refs. [11–13], the fictitious magnetic field is a real physical quantity, and its role is significant in the construction of the alternative mechanism of high- T_c superconductivity.

At the end of this section, one can say that the bosonic ground state nature of the arbitrary $2D$ quantum system is the intrinsic fundamental property of the two dimensionality, which originates from its topology. In the light of this finding, the appearance of single bosons in the experiment of Gomes *et al.* [1] and discussed in the previous section might be not occasional. Another important qualitative issue, which leads from a result of [1] experiment, is in the following. The random positions in the real space of the observed pairs totally exclude any mechanism for the pair formation. Since occasionally positioned in this space coherent excitations (phonons, magnons or other quasi-particles), which create pairs, are problematic, if the system is homogenous. The last observation deduced from Gomes *et al.* paper is the fundamental argument for the justification of the single hole nature of the cuprate physics.

IV. ORIGIN OF UEMURA RELATION

Now, it is widely accepted (see Ref. [34]) that the Uemura relation (UR), the linear dependence of T_c on concentration of charge carriers, originally observed in Refs. [35] and [36] for underdoped cuprate, bismuthate, organic, Chevrel-phase and heavy-fermion superconductors, survives also for extended class of other superconductors and has a fundamental universal character. There is no doubt that this relation together with other empirical Home's law, Ref. [37], for cuprate and conventional (but except the molecular, Ref. [38]) superconductors plays an important role for the construction of the mechanism of superconductivity in these materials and can even be a source for discovering fundamental properties of the underlying physics. It is worth to remind that the Home's law relates a superfluid density (charge concentration) to the electric conductivity of the normal state nearly above T_c and T_c itself.

Recently, there was observed a deviation from the UR into sublinear scale, in which T_c had the dependence on carrier concentration with power less than unit (more exactly with power close to $1/2$), for the particular $YBa_2Cu_3O_y$ cuprate (see Ref. [39]

and references therein) and in $Y_{0.8}Ca_{0.2}Ba_2Cu_3O_{7-\delta}$, $Bi_2Sr_2CaCu_2O_{8+\delta}$ and $La_{2-x}Sr_xCuO_4$ copper oxides, Ref. [40]. In the second case the deviation was more evident for doping close to and beyond the optimal one. The additional deviation from the linear concentration dependence of T_c , with the power of concentration slightly greater than unit (with power $3/2$), was reported in Ref. [38] for quasi- $2D$ molecular superconductors.

However, the experimental data have indicated the prominent UR for samples with nearly $2D$ geometry: Ref. [41] for ultrathin $La_{2-x}Sr_xCuO_4$ and Ref. [42] for very thin $NdBa_2Cu_3O_{7-\delta}$. The problem with uncertainty of power of the carrier concentration was resolved in the remarkable and unprecedented on precision experimental investigation, Ref. [43], of T_c as function of carrier concentration. Authors of Ref. [43] have studied the power of the dependence as function of number of CuO_2 atoms containing $a - b$ layers for $Y_{1-x}Ca_xBa_2Cu_3O_{7-\delta}$ cuprate. Varying this number from 40 down to 2, they observed the changing the power of concentration from $1/2$ to unit, thus revealing the obvious relation of UR to the two-dimensionality of the system. Motivated by this observation, in the present section we investigate the possible role of the fermion bosonization, which is a result of the topology of $2D$, to the origin of UR.

In our previous work [27] we have derived an analytic expression for the ground state energy of the homogeneous $2D$ anyon gas with the Coulomb interaction. This was done for all values of the statistics parameter ν and mean distance between particles r_0 by flattening out the confining potential with a simultaneous increase of the particle number N , but fixed areal density, to obtain the infinite size system, i.e., the thermodynamic limit. It has been achieved by the redefining the strength ω_0 of the harmonic potential in the Hamiltonian, Eq. (1), such that it vanishes with increasing N .

Applying the relationship $r_0 \approx a/x^{1/2}$, where $a \approx 3.8\text{\AA}$ (see Sec. II), we do an estimate values of r_0 , expressed in Bohr radius a_B unit ($r_s = r_0/a_B$), corresponding the doping interval $x_{c1} \leq x \leq x_{c2}$. One obtains $13.12 \leq r_s \leq 32.14$. For this interval of r_s we have obtained in Ref. [27] the expression

$$\mathcal{E}(\nu, r_s) = \frac{E(\nu, r_s)}{NRy} = E_{WC} + \frac{7\nu E_{WC}^2}{3c_{WC}^2} \quad (14)$$

for the ground state energy per particle of the Coulomb interacting anyon gas. Here, Ry is the Rydberg energy unit and for large r_s the ground state energy does not depend on statistics and equals to the energy of the classical $2D$ Wigner crystal [44], $E_{WC} = -c_{WC}^{2/3}/r_s$ with $c_{WC}^{2/3} = 2.2122$.

Taking into account from the previous section that the excited state of the $2D$ system is fermionic and the ground state is bosonic, one can write the explicit expression for an energy gap between these two states

$$\Delta(r_s) = \mathcal{E}(\nu = 1, r_s) - \mathcal{E}(\nu = 0, r_s) = \frac{7E_{WC}^2}{3c_{WC}^2}. \quad (15)$$

The meaning of this expression is that to become the fermion the boson should gain the energy $\Delta(r_s)$. Substituting in Eq. (15) the expression for E_{WC} and introducing the $2D$ density $n = 1/(\pi r_0^2)$ one derives

$$\Delta(n) = \frac{7\pi n a_B^2}{3c_{WC}^{2/3}}. \quad (16)$$

Since the critical temperature T_c is proportional to $\Delta(n)$, one can conclude that the $2D$ topology driven bosonization of fermions may explain the UR for variety superconductors, whose physics is quasi - two dimensional.

In Ref. [28], using the expression of $\Delta(n)$ for optimal doping, we have obtained the values of the maximal temperature $T_{c,max}$ of the doping-temperature phase diagram for hole and electron doped cuprates, which were close to experimental ones.

V. CONCLUSION

Summarizing the paper, we have succeeded in understanding the following constituents of the doping-temperature phase diagram of the hole doped copper oxides: (i) the first and second critical dopings have been a result of emergence and disappearance of the single hole boson percolation lines, respectively; (ii) the disappearance of the percolation lines leads to the end of the PG bulk bosonic property or to the end of Nernst effect signals; (iii) the fact that the PG boundary was a bound, where the single hole bosons disappear, confirmed

by Ref. [1]. Our findings are consistent with the recent observation [45] of the superconducting phase consisted of the array of nanoclusters embedded in the insulating matrix and of percolative transition to this phase from the normal phase in $YBa_2Cu_3O_{6+\delta}$. Superconducting islands introduced in insulating background have been used for the interpretation of the superconductor-insulator transition in $Bi_2Sr_{2-x}La_xCaCu_2O_{8+\delta}$ compound [46]. In a recent paper [47] (see also [12]) a significant role of the percolation of elementary structural plaquettes on universal properties of cuprates has been established. Using $3D$ percolation mechanism the authors of Ref. [47] succeeded in explanation of the T_c phase diagram, room-temperature thermopower, neutron spin resonance, and STM incommensurability.

We have presented justification in the microscopic treatment of the appearance of single bosons. In rigorous derivation we have obtained the bosonization of $2D$ fermions, thus proposing the bosonic ground state for any $2D$ quantum systems. The crucial role in our consideration is assigned to the concept of anyons. The UR for $2D$ superconductors has been also understood according to the fermion bosonization approach. The boson and fermion mixing nature of PG region, derived from experiment [1], is consistent with our treatment and description of low temperature non-Fermi liquid heat conductivity and entropy [48].

VI. ACKNOWLEDGEMENTS

The work is partially supported by Korean Research Foundation (Grant KRF-2006-005-J02804).

-
- [1] K. K. Gomes *et al.*, Nature 447 (2007) 569.
[2] S. H. Pan *et al.*, Nature 413 (2001) 282.
[3] Y. Wang, L. Li, and N. P. Ong, Phys. Rev. B 73 (2006) 024510.
[4] V. J. Emery and S. A. Kivelson, Nature 374 (1995) 434.
[5] J. Corson *et al.*, Nature 398 (1999) 221; Z. A. Xu *et al.*, Nature 406 (2000) 486; Y. Wang *et al.*, Phys. Rev. Lett. 95 (2005) 247002.
[6] J. L. Tallon and J. W. Loram, Physica C 349 (2001) 53.
[7] M. Vershinin *et al.*, Science 303 (2004) 1995; T. Hanaguri *et al.*, Nature 430 (2004) 1001; K. McElroy *et al.*, Phys. Rev. Lett. 94 (2005) 197005.
[8] N. Timusk and B. Statt, Rep. Prog. Phys. 62 (1999) 61.
[9] C. Howald, P. Fournier, and A. Kapitulnik, Phys. Rev. B 64 (2001) 100504(R).
[10] K. McElroy *et al.*, Science 309 (2005) 1048.
[11] H. Koizumi, J. Phys. A 43 (2010) 354009.
[12] H. Koizumi, J. Phys. Chem. A 113 (2009) 3997.
[13] H. Koizumi, J. Phys. Soc. Jpn. 77 (2008) 034712.
[14] M. A. Kastner, R. J. Birgeneau, G. Shirane, and Y. Endoh, Rev. Mod. Phys. 70 (1998) 897.
[15] R. B. Laughlin, in *The Quantum Hall Effect*, Edited by R. E. Prange and S. M. Girvin, (Springer-Verlag, New York, 1987).
[16] L. N. Smith and C. J. Lobb, Phys. Rev. B 20 (1979) 3653.
[17] A. Weinrib, Phys. Rev. B 26 (1982) 1352.
[18] J. M. Leinaas and J. Myrheim, Nuovo Cimento Soc. Ital. Fis., B 37 (1977) 1.
[19] F. Wilczek, Phys. Rev. Lett. 48 (1982) 1144.
[20] F. Wilczek, *Fractional Statistics and Anyon Superconductivity* (World Scientific, Singapore, 1990).
[21] S. Forte, Rev. Mod. Phys. 64 (1992) 193; R. Iengo and K. Lechner, Phys. Rep. 213 (1992) 179; *Quantum Hall Effect*, edited by M. Stone (World Scientific, Singapore, 1992).
[22] A. Lerda, *Anyons* (Springer-Verlag, Berlin, 1992).
[23] A. Khare, *Fractional Statistics and Quantum Theory*, 2nd ed. (World Scientific, Singapore, 2005).
[24] A.Yu. Kitaev, Ann. Phys. (N.Y.) 303 (2003) 2.
[25] G. Dunne, A. Lerda, S. Sciuto and C. A. Trugenberger,

- Nucl. Phys. B 370 (1992) 601.
- [26] B. Abdullaev, G. Ortiz, U. Rössler, M. Musakhanov, and A. Nakamura, Phys. Rev. B 68 (2003) 165105.
- [27] B. Abdullaev, U. Rössler, and M. Musakhanov, Phys. Rev. B 76 (2007) 075403.
- [28] B. Abdullaev, in *Trends in Boson Research*, Editor A. V. Ling (Nova Science Publishers, N. Y., 2006), pp. 139-161, cond-mat/0507500; B. Abdullaev and C.-H. Park, J. Korean Phys. Soc. 49 (2006) S642, cond-mat/0404668.
- [29] Y. -S. Wu, Phys. Rev. Lett. 53 (1984) 111, Erratum ibid 53 (1984) 1028; R. B. Laughlin, Phys. Rev. Lett. 60 (1988) 2677.
- [30] A. Comtet, J. McCabe and S. Ouvry, Phys. Lett. B 260 (1991) 372.
- [31] J. McCabe and S. Ouvry, Phys. Lett. B 260 (1991) 113; A. Dasnières de Veigy and S. Ouvry, ibid. 291 (1992) 130; Nucl. Phys. B 388 715 (1992); D. Sen, ibid. 360 (1991) 397; J. Y. Kim, Y. S. Myung, and S. H. Yi, Phys. Lett. B 331 (1994) 347.
- [32] R. Chitra and D. Sen, Phys. Rev. B 46 (1992) 10923.
- [33] L. D. Landau, and E. M. Lifshitz, *Quantum Mechanics, Non-Relativistic Theory* (Pergamon Press, Oxford, 1977) § 65.
- [34] J. Zaanen, Nature 430 (2004) 512.
- [35] Y. J. Uemura *et al.*, Phys. Rev. Lett. 62 (1989) 2317.
- [36] Y. J. Uemura *et al.*, Phys. Rev. Lett. 66 (1991) 2665.
- [37] C. C. Homes *et al.*, Nature 430 (2004) 539.
- [38] F. L. Pratt and S. J. Blundell, Phys. Rev. Lett. 94 (2005) 097006.
- [39] J. E. Sonier *et al.*, Phys. Rev. B 76 (2007) 134518.
- [40] J. L. Tallon *et al.*, Phys. Rev. B 68 (2003) 180501.
- [41] A. Rüfenacht *et al.*, Phys. Rev. Lett. 96 (2006) 227002.
- [42] D. Matthey *et al.*, Phys. Rev. Lett. 98 (2007) 057002.
- [43] I. Hetel, T. R. Lemberger, and M. Randeria, Nature Phys. 3 (2007) 700.
- [44] L. Bonsal and A. A. Maradudin, Phys. Rev. B 15 (1977) 1959.
- [45] S. Yu. Gavrilkin, O. M. Ivanenko, V. P. Martovitskii, K. V. Mitsen, and A. Yu. Tsvetkov, Arxiv: 0909.0612.
- [46] S. Oh, T. A. Crane, D. J. Van Harlingen, and J. N. Eckstein, Phys. Rev. Lett. 96 (2006) 107003.
- [47] J. Tahir-Kheli and W. A. Goddard, J. Phys. Chem. Lett. 1 (2010) 1290.
- [48] B. Abdullaev, C. -H. Park, and K. -S. Park, cond-mat/0703290.